Imaging characteristics of choroid plexuses in pre-symptomatic multiple sclerosis: a retrospective study

Vito a G Ricigliano, Emilie Poirion, Annalisa Colombi, Yazdan Panah, Andrea Lazzarotto, Emanuele Morena, Elodie Martin, Michel Bottlaender, Benedetta Bodini, Danielle Seilhean, et al.

Imaging characteristics of choroid plexuses in pre-symptomatic multiple sclerosis: a retrospective study.

Vito A. G. Ricigliano, MD, PhD[1,2]; Céline Louapre, MD, PhD[1,3]; Emilie Poirion, PhD[1,4]; Annalisa Colombi, MD[1]; Arya YAZDAN PANAH, MSc[1]; Andrea Lazzarotto, MD[1,2]; Emanuele Morena, MD[1]; Elodie Martin, PhD[1]; Michel Bottlaender, MD, PhD[5]; Benedetta Bodini, MD, PhD[1,2]; Danielle SEILHEAN, MD[1,6]; Bruno Stankoff, MD PhD[1,2]

Corresponding Author:

Bruno Stankoff

bruno.stankoff@aphp.fr

Affiliation Information for All Authors: 1. Sorbonne Université, Paris Brain Institute, ICM, CNRS, Inserm, 75013 Paris, France; 2. Neurology Department, St Antoine Hospital, APHP-Sorbonne, 75012 Paris, France; 3. Neurology Department, Pitié-Salpêtrière Hospital, APHP-Sorbonne, 75013 Paris, France; 4. Service dImagerie Médicale, Hôpital Fondation Adolphe de Rothschild, 75019 Paris, France; 5. Université Paris-Saclay, CEA, CNRS, Inserm, BioMaps, Service Hospitalier Frédéric Joliot, 91400 Orsay, France; 6. Neuropathology Department, Pitié-Salpêtrière Hospital, APHP-Sorbonne, 75013 Paris, France

Abstract

Background and objectives: Recent imaging studies have suggested a possible involvement of choroid plexus (CP) in multiple sclerosis (MS). Here, we investigated whether CP changes are already detectable at the earliest stage of MS, preceding symptom onset.

Methods: The study is a retrospective analysis of 27 pre-symptomatic MS subjects, 97 clinically definite MS (CDMS) patients and 53 healthy controls (HC) who underwent a cross-sectional 3T-MRI acquisition; of which, 22 MS, 19 HC and one pre-symptomatic MS (evaluated 8 months before conversion to CDMS) also underwent translocator protein (TSPO) ^{18}F-DPA-714 PET and were included in the analysis. CPs were manually segmented on 3DT1-weighted images for volumetric analysis. CP ^{18}F-DPA-714 uptake, reflecting inflammation, was calculated as the average standardized uptake value (SUV). Multivariable regressions adjusted for age, sex, ventricular and brain volume were fitted to test CP volume differences between pre-symptomatic subjects and MS or HC. For the pre-symptomatic case who also had ^{18}F-DPA-714-PET, CP SUV differences with MS and HC were assessed through Crawford-Howell tests. To provide further insight into the interpretation of ^{18}F -DPA-714-PET uptake at the CP level, a *post-mortem* analysis of CPs in MS *versus* HC was performed to characterize the cellular localization of TSPO expression.

Results: Compared with HC, pre-symptomatic MS subjects had 32% larger CPs (ß=0.38, p=0.001), which were not dissimilar to MS CPs (p=0.69). Moreover, in the baseline scan of the pre-symptomatic case who later on developed MS, TSPO PET showed 33% greater CP inflammation *versus* HC (p=0.04), while no differences in ^{18}F-DPA-714 uptake were found in parenchymal regions *versus* controls. CP *post-mortem* analysis identified a population of CD163+ mononuclear phagocytes expressing TSPO in MS, possibly contributing to the increased in ^{18}F-DPA-714 uptake.

Discussion: We identified an imaging signature in CPs at the pre-symptomatic MS stage using MRI; additionally, we found an increased CP inflammation with PET in a single pre-symptomatic patient. These findings suggest a role of CP imaging as an early biomarker and argue for the involvement of the blood-CSF barrier dysfunction in disease development.

Trial registration numbers: APHP-20210727144630, EudraCT-Number: 2008-004174-40; ClinicalTrials.gov: NCT02305264, NCT01651520, NCT02319382.

Introduction

Choroid plexuses (CPs) are central nervous system (CNS) structures involved in cerebrospinal fluid (CSF) production and immunosurveillance.[1] They regulate the bidirectional exchange between the blood and the CSF, forming the so-called blood-CSF barrier (BCSFB).[2-3] Their structural and functional alterations may contribute to the pathophysiology of immune-mediated CNS diseases like multiple sclerosis (MS). We previously described, in a study combining magnetic resonance imaging (MRI) and inflammatory positron emission tomography (PET) in patients with MS *versus* healthy controls (HC), that CPs have greater volume and higher translocator protein (TSPO) expression at the inflammatory phase of the disease, possibly reflecting increased macrophage/microglia infiltration.[4] We demonstrated that CP enlargement correlated with imaging metrics of parenchymal inflammation and with relapse rate in relapsing-remitting MS (RRMS). Recently, the role of CP volumetric increase as neuroinflammatory marker over time has been corroborated in a translational study.[5]

In the experimental autoimmune encephalitis (EAE) model, CPs allow the initial lymphocytic infiltration into the CNS.[6-7] In human pathology, this early, pre-symptomatic phase of the disease is often referred to as radiologically isolated syndrome (RIS).[8-9] This entity corresponds to patients with radiological signs of MS without neurological events, but with a higher risk of clinical conversion for males, aged <37 years, with cervical/thoracic spinal cord lesions and gadolinium-enhancing lesions.[10-11] Thus far, however, definite predictive imaging markers at the pre-symptomatic stage are lacking, and a possible involvement of CPs at this early subclinical phase of MS has never been investigated *in vivo*.

To this aim, we performed a 3 Tesla MRI volumetric analysis of CPs in a cohort of 27 subjects with pre-symptomatic MS (26 RIS, and one pre-symptomatic MS woman with two WM lesions, one of which in a MS-typical CNS location) *versus* 97 patients with MS and 53 HC. Moreover, we measured CP inflammation with TSPO ^{18}F-DPA-714-PET in one subject with pre-symptomatic MS who converted to clinically defined MS 8 months later, and compared results with 22 MS and 19 HC. Finally, we characterized the cellular localization of CP TSPO expression in the disease on *post mortem* samples.

Methods

Subjects

Twenty-six subjects fulfilling the 2009 RIS diagnostic criteria,[8] followed between September 2013-January 2021, and validated by the RIS International Consortium, for whom MRI scans with non-enhanced 3D-T1-weighted sequences were available, were retrospectively selected from our Neurology clinics of Saint-Antoine and Pitié-Salpêtrière Hospital in Paris, France. Clinical history, CSF positivity (either high IgG index or positive oligoclonal bands),[11] conversion to MS and follow-up duration (months) since the analyzed MRI were collected until august 2021. Consent according to the French legislation for non-interventional research was obtained from all subjects (APHP-20210727144630). In addition, a 30-year-old female with pre-symptomatic MS, originally included as healthy volunteer in a protocol combining 3T-MRI and ^{18}F-DPA-714-PET for the study of innate immune cell activation in patients with MS *versus* HC (ClinicalTrials.gov: NCT02305264),[12] but then classified as pre-symptomatic MS, was added to the studied cohort. After genotyping of the rs6971 polymorphism of *TSPO* gene,[13] she was classified as high-affinity binder (HAB).

A retrospective convenience series of 97 patients with MS (61 relapsing-remitting, RRMS, and 36 progressive, PMS) and 53 HC from four prospective cross-sectional studies performed between 2009-2017 (EudraCT-Number: 2008-004174-40; ClinicalTrials.gov: NCT02305264, NCT01651520, NCT02319382)[4,14] was used to collect MRI data. From this population, 37 patients and 28 HC also underwent ^{18}F-DPA-714 PET at study entry (ClinicalTrials.gov: NCT02305264, NCT02319382).[12,14] After rs6971 genotyping, 22 patients with MS and 19 HC were classified as HAB for *TSPO* polymorphism and kept for further analysis (NCT02305264, NCT02319382). Written informed consent was obtained from all participants according to the Declaration of Helsinki and the studies were approved by the local ethic committees.

Standard Protocol Approvals, Registrations, and Patient Consents

Participant consent according to the French legislation for non-interventional research was obtained from all pre-symptomatic MS subjects (APHP-20210727144630), and from the subjects with MS and healthy controls enrolled in the four prospective cross-sectional PET-

MRI studies (EudraCT-Number: 2008-004174-40; ClinicalTrials.gov: NCT02305264, NCT01651520, NCT02319382).

Image acquisitions

All subjects underwent a 3T-MRI exam including the following sequences: 3D T1-weighted magnetization-prepared rapid gradient echo (3D-T1 MPRAGE), 2D turbo spin-echo T2-weighted (T2-w), and/or T2 fluid attenuated inversion recovery (FLAIR). Sequence parameters for the research protocols were: i) 3D-T1 MPRAGE: repetition time (TR)/echo time (TE): 2300/2.98 ms, inversion time: 900 ms, resolution: 1.0x1.0x1.1mm^3; ii) T2-w: TR/TE: 4100/83 ms, resolution: 0.9x0.9x3.0mm^3; iii) FLAIR: TR/TE 8880/129ms, resolution :0.9x0.9x3.0mm^3.

^{18}F-DPA-714 PET exams were performed on a 3D high-resolution research tomograph (HRRT; CPS Innovations, Knoxville, TN) with a 31.2 cm transaxial and 25.5 cm axial field of view. After a transmission scan using a ^{137}Cs point source, a 1-minute intravenous bolus injection of ^{18}F-DPA-714 initiated the 90-minute emission scan. Images were reconstructed using the 3D ordinary Poisson ordered subset expectation maximization algorithm. An additional smoothing filter implementing the point spread function was performed on the reconstructed images to achieve an intra-slice spatial resolution of ~2.5mm full width at half maximum. The resulting dynamic PET images consisted of: six 1min frames for the initial 6 minutes (6x1), followed by 7x2-, and 14x5-minute frames, with a voxel size of 1.22x1.22x1.22mm^3.

Post-processing

In subjects with MS and pre-symptomatic MS, white matter (WM) lesions were contoured on T2-weighted images with reference to FLAIR images using Jim (v6.0, http://www.xinapse.com/). Binary lesion masks were aligned to 3D-T1 scans with FLIRT (v5.0.9, http://fsl.fmrib.ox.ac.uk/),[15] followed by lesion filling. FreeSurfer (v6.0, http://surfer.nmr.mgh.harvard.edu/)[16] was then used on the 3D-T1 to estimate total intracranial volume (TIV) and to segment gray matter, WM and CSF, with manual corrections when necessary.

The CPs of the lateral ventricles were manually segmented by trained neurologists on the three planes of the 3D-T1 using ITK-SNAP (v3.8.0, http://www.itksnap.org/) (**Figure 1A)**,[17] and their volume was calculated. Ventricles, whole brain, cortex and WM were extracted as additional regions of interest (ROIs) from T1-w scans using FreeSurfer.[16] In patients with MS and pre-symptomatic subjects, two other ROIs were selected: (i) T2-w lesions; (ii) normal-appearing WM (NAWM), defined as the WM without T2-weighted lesions. Volumes were divided by TIV to obtain the corresponding normalized value.

From PET scans, reconstructed dynamic data were realigned for motion correction using SPM (v8, https://www.fil.ion.ucl.ac.uk/spm/). In particular, the first PET frame was excluded as it did not contain enough spatial information to be correctly aligned. Motion correction was performed with a two-step procedure: all frames were first aligned to the second frame through a rigid transformation, and were then registered to the mean of the frames obtained after the first realignment. Voxel-wise ^{18}F-DPA-714 distribution volume ratio (DVR) parametric maps, reflecting parenchymal ^{18}F-DPA-714 uptake, were obtained using Logan graphical method based on reference region.[18] Cortical, WM (NAWM) and T2-w lesions ROIs were then aligned to the corresponding DVR maps using FLIRT[14] to extract mean DVR values. Choroid plexus ^{18}F-DPA-714 uptake was defined as the average standardized uptake value (SUV) inside the CPs. The use of SUV instead of DVR at this level relies on the fact that the assumptions for Logan graphical analysis were not respected in this case. SUV maps of ^{18}F-DPA-714 were calculated from the frames between 60 and 90 minutes of acquisition ($SUV_{60\text{-}90}$) as the radioactivity concentration divided by injected dose per body mass. Mean ^{18}F-DPA-714 $SUV_{60\text{-}90}$ in the CPs was extracted for each subject by overlapping the CP masks to the SUV maps, after performing CP partial volume correction with the single target correction (STC) method in PETPVC (v1.2.0-b, https://github.com/UCL/PETPVC).[4,19]

Post mortem analysis

CP post-mortem samples were obtained from the French National BrainBank Donation Program NeuroCEB. Samples were obtained from 3 patients with MS with severe disease (2 males, 1 secondary progressive/2 primary progressive, age: 54±11 years, disease duration: 29±10 years) and 2 non-MS controls (2 males, 1 epilepsy and one HC, age: 63±10). Half of the brain was fixed by immersion in 4% formaldehyde; formalin-fixed samples were embedded in paraffin and cut at a 3µm thickness. Selected sections were immunostained

using a Ventana BenchMark stainer (Roche™, Tucson, AZ, USA). Diaminobenzidine and alkaline phosphatase were used as chromogens. Pretreatment and antibodies used for immunostaining are in **Table 1**.

Statistical analysis

STATA (v14.0, https://www.stata.com/) and R (http://www.R-project.org/) were used, considering two-sided $p<.05$ as significant.

The sample size estimated for showing a CP enlargement in RIS was calculated based on an expected 25% increase (inferior to the 35% found in patients in our previous study)[4] in mean CP volume compared with HC. Setting power=80%, alpha=0.05 and enrollment ratio 1:2, a minimum of 20 pre-symptomatic MS subjects was necessary to detect a $\geq$ 25% inter-group difference in CP volume.

Wilcoxon-Mann-Whitney and Fisher's tests were used as appropriate for age and sex differences. Shapiro-Wilk normality test was performed to check the distribution of volumetric data. Inter-group differences in CP, ventricular, brain parenchymal and total intracranial volume were assessed through unpaired t-tests. Pearson's r was used for the correlation between CP and ventricular volume in pre-symptomatic MS subjects. Multivariable linear regression models adjusted for age and sex were used to test differences in ventricular, whole brain parenchymal volume and TIV (dependent variables) between pre-symptomatic MS and MS or HC (independent binary variables). The same models, additionally adjusted for ventricular and whole brain parenchymal volume, were fitted to test differences in TIV-normalized CP volume: i) between pre-symptomatic MS and MS or HC; ii) within pre-symptomatic MS, between CSF-positive *versus* CSF-negative subjects, and between converters to MS *versus* non-converters (additionally accounting for follow-up length).

In the subgroup analysis on the PET cohort, differences in age, CP volume, mean ^{18}F-DPA-714 DVR and CP ^{18}F-DPA-714 $SUV_{60\text{-}90}$ between the pre-symptomatic case and MS or HC were assessed through Crawford-Howell tests.

Data availability

Anonymized data are available upon reasonable request from any qualified investigator.

Results

CPs are larger in subjects with pre-symptomatic MS

The pre-symptomatic group (n=27) was not different from MS and HC in mean age (years, pre-symptomatic MS: 42±11, MS: 42±12, HC: 42±14.4, p=0.72 and p=0.73, respectively) or sex (women, pre-symptomatic MS: 17, MS: 49, HC: 28, p=0.20 and p=0.48, respectively). Lumbar puncture was performed in 24 pre-symptomatic MS subjects, of which 11 had positive CSF (either high IgG index or positive oligoclonal bands; 46%). Median follow-up from the analyzed MRI scan was 30 (7-95) months. Conversion to MS occurred in five subjects (18.5%).

When assessing volumetric differences between the pre-symptomatic MS cohort and either MS or HC, mean CP volume was 32% higher in the pre-symptomatic MS group *versus* HC (pre-symptomatic MS, mean normalized CP volume ± standard deviation, SD: $14.9\pm5.2x10^{-4}$, HC, mean normalized CP volume ± SD: $11.3\pm3.9x10^{-4}$, $p<0.001$). On the contrary, there was no difference in CP volume between pre-symptomatic MS and MS (MS, mean normalized CP volume ± SD: $15.9\pm4.5x10^{-4}$, p=0.35) (**Figure 1B**). A significant difference between the pre-symptomatic MS group and HC was also found in ventricular size (pre-symptomatic MS, mean normalized ventricle volume ± SD: $16.4\pm7.1x10^{-3}$, HC, mean normalized ventricle volume ± SD: $12.9\pm4.7x10^{-3}$, p=0.009), but not in TIV or brain parenchymal volume (**Table 2**). In the pre-symptomatic cohort, CP volume correlated with ventricular volume (r=0.55, p=0.003), as already described for MS.[4] After adjusting for the ventricle size, CPs were still larger in RIS than HC (ß=0.38, regression coefficient=$3.76x10^{-4}$, 95% confidence interval [CI]=$1.54x10^{-4}$:$5.98x10^{-4}$, p=0.001). There was no statistical difference in the CP volume adjusted for ventricle size between RIS and MS (p=0.69). In the pre-symptomatic MS cohort, CP volume in subjects with a CSF-positive pattern (defined as either high IgG index or positive oligoclonal bands, n=11) was similar (mean normalized CP volume ± SD: 13.1 ± 3.7 x 10^{-4}), compared to subjects with CSF-negative pattern (n=13, mean normalized CP volume ± SD: 16.7 ± 6.5 x 10^{-4}, p=0.20). Mean choroid plexus size did not significantly differ between RIS subjects who converted to MS during follow-up (n=5, mean normalized CP volume ± SD: 16.1 ± 3.8 x 10^{-4}) and those who did not convert (n=22, mean normalized CP volume ± SD: 14.7 ± 5.5 x 10^{-4}, p=0.74).

Higher CP DPA uptake in a single pre-symptomatic patient

The pre-symptomatic MS woman who underwent both MRI and PET had two WM hyperintensities (periventricular and deep WM) on baseline MRI, allowing to classify her as pre-symptomatic MS. Eight months later, she experienced a first clinical event, together with the appearance of a new gadolinium-positive lesion located in the left frontal white matter and a new gadolinium negative lesion in the right juxta cortical white matter, leading to the diagnosis of MS according to the McDonald criteria 2010. At baseline, she did not differ from MS or HC for age (p=0.08, and p=0.1). Her CP volume was 77% larger than the mean volume measured in HC (**Figure 1C**, case's normalized CP volume: $20x10^{-4}$, p=0.008), being greater than the one measured in 98.4% of HC (95%CI=$9.16x10^{-4}$:0.04), and similar to the mean volume of patients with MS (p=0.09) (**Figure 1D**). Looking at TSPO PET (**Figure 2A**), her ^{18}F-DPA-714 SUV_{60-90} within CPs was 33% higher than in HC (case's CP SUV_{60-90}: 0.794, mean CP SUV_{60-90} ± SD of HC: 0.596±0.13, p=0.04), being greater than the one measured in 92% of HC (95%CI=$6.35x10^{-3}$:0.17) (**Figure 2B,D**), but did not differ from the CP SUV_{60-90} of the MS group (mean CP SUV_{60-90} ± SD of MS: 0.887±0.22, p=0.17) (**figure 2C,E**). No significant differences between the pre-symptomatic MS and HC were found for ^{18}F-DPA-714 DVR in the cortex (case's cortex DVR: 1.41, mean cortex DVR ± SD of HC: 1.32±0.13, p=0.13), in the WM (case's WM DVR: 0.96, mean WM DVR ± SD of HC: 0.89±0.08, p=0.10) or in T2-w hyperintensities compared with HC's WM (case's DVR in T2-w hyperintensities: 0.98, p=0.07).

TSPO is expressed by epithelial cells and CD163+ macrophages in the CPs of patients with MS

In CPs of patients with an history of active MS and non-MS controls, a high TSPO expression was found in epithelial cells. CPs of patients with MS also showed an excess of CD163+ macrophages compared with controls (**Figure 3A-B**). Double immunostaining identified a TSPO+ pool which was also positive for the monocyte/macrophage-specific marker CD163 in MS only (**Figure 3C-F**). No cells co-expressing TSPO with either the T-lymphocyte marker CD3, the B-lymphocyte marker CD20, or the peripheral macrophage marker CD68 were identified.

Discussion

We investigated the imaging signature of choroid plexuses at the preclinical stage of MS *versus* healthy controls through a combination of MRI and ^{18}F-DPA-714 TSPO-PET. We provide evidence that CPs are larger (32% increase) and have higher ^{18}F-DPA-714 uptake (33% increase in the single patient included in the analysis) in pre-symptomatic subjects compared with HC. CP histology from patients with MS and non-MS controls showed a population of CD163+/TSPO+ macrophages, detected only in MS, which may contribute, at least partly, to the difference in TSPO expression between the two conditions.

Beyond CSF production, CPs regulate immune cell trafficking between the blood and the CNS, involving CP mononuclear phagocytes in this complex homeostasis.[20-21] In MS, the neuroinflammatory component is not currently detected by clinical MRI, but can be quantified using PET with TSPO tracers such as ^{18}F-DPA-714.[22] We recently described *in vivo* a higher CP ^{18}F-DPA-714 uptake in MS *versus* controls, this difference being particularly pronounced in RRMS.[4] Here, we extend this finding by showing similar changes in the CPs of preclinical MS, suggesting that a BCSFB deregulation could be among the earliest processes characterizing MS pathophysiology. Of note, only CPs, but not the brain parenchyma, showed increased ^{18}F-DPA-714 binding in the pre-symptomatic patient, mimicking the sequence of events characterizing EAE, in which inflammation within CPs precedes the parenchymal infiltrate and demyelination.[6] Neuropathology has described an increased density of antigen presenting cells, leukocyte infiltration and overexpression of proinflammatory adhesion molecules in MS CPs.[23-24] In the *post mortem* analysis of CPs from patients with a previous severe course of the disease and from controls, we observed, as expected, that TSPO was expressed by epithelial and vascular cells in all subjects,[25] but an additional expression by CD163+ macrophages selectively characterized MS, this difference potentially explaining their higher ^{18}F-DPA-714 uptake. Interestingly, this TSPO expression was restricted to CD163+ cells, and was not detected on CD3+ or CD20+ lymphocytes, nor on CD68+ monocytes, suggesting a selective increase in perivascular CPs macrophages involved in antigen presentation in MS.[20,26] Unfortunately, lacking pathological samples, it was not possible to explore whether similar alterations also occur at the earliest MS stages, and a more heterogeneous TSPO expression by distinct subsets of monocytes in this phase cannot be excluded. In the case reported here, a first relapse occurred few months after the PET

evidence of inflamed CPs, and future studies applying TSPO-PET at the preclinical stage will be of outstanding interest to decipher whether the inflammatory status of CPs could be predictive of conversion towards defined MS.

We previously demonstrated correlation between ^{18}F-DPA-714 uptake in the CPs and their increased volume on MRI in RRMS,[4] arguing for the possibility to use CP enlargement as a proxy of CP inflammation. A recent study has further reinforced the relationship between CP enlargement, their inflammatory status, and parenchymal inflammation.[5] Taken together, these results attest that CP volumetric analysis could represent a promising *in-vivo* biomarker of MS neuroinflammation.[5] In accordance with this hypothesis, CP enlargement in pre-symptomatic MS confirms that this imaging signature is an early phenomenon along the disease course. Whether CP imaging modifications are stable or fluctuate with the inflammatory phases of the disease remains to be addressed. Focusing on RIS may offer complementary assets to: i) disentangle the temporal, and possibly causal, relationship between CP alterations and symptom onset; ii) follow the natural history of CP modifications without the bias of treatment, and estimate the potential impact of disease-modifying therapies, once these are introduced at the defined MS stage; iii) characterize the involvement of CPs in the physiopathology of lesion formation and fate, investigating the initial inflammatory infiltration into the CNS, the BCSFB disruption and the relationship with CSF inflammatory markers.

Another important question to be addressed is to what extent CP volumetric and inflammatory alterations are specific for MS with respect to other acute or chronic inflammatory/infectious disorders of the CNS. This goes beyond the scopes of the present study, but very recent findings suggest that CP enlargement is detected in MS in contrast to optic neuromyelitis,[27] pointing at a possible specificity of choroid plexus modifications in relation to the respective pathogenesis.

Given the low cost and higher accessibility of MRI,[28] CP volumetric analysis could become an easy technique to assess this imaging signature on a larger scale. To this aim, the development of artificial intelligence-based methods for automatic CP segmentation,[29-30] and the integration of additional MRI sequences for perfusion,[31] could allow a time- and cost-sparing evaluation of CP modifications, compared with PET.

This study has potential limitations. The RIS group was collected in a clinical setting, producing heterogeneity of MRI scanners and parameter acquisitions. Nonetheless, the ability to identify CP volume differences even in the real-world prompts for the possible application of this metric outside of standard research protocols. Additionally, the pre-symptomatic cohort, despite being large enough to detect inter-group differences, was relatively small. This may have affected the absence of detectable CP volume differences between CSF-positive and -negative subjects, or converters to MS *versus* non-converters, given the low proportion of people who developed MS over time.[10] Therefore, studies on larger populations and longer follow-up periods are necessary to better define the impact of CP modifications on disease conversion. Another limitation concerns the post-mortem data presented here. The similar ^{18}F-DPA-714 PET changes found in the CPs of the pre-symptomatic subject and of patients with more advanced MS may suggest that they had an identical underlying pathological substrate, but we lacked a direct post-mortem analysis of CPs at the RIS stage to formally demonstrate this. Of note, however, among early, newly diagnosed subjects with MS, an involvement of a CD163 positive macrophage/microglial population was described, [32] echoing what found in more advanced stages,[33] supporting the hypothesis of an early contribution of this macrophage population at the RIS stage.

To note, our histology data show that epithelial cells are a major source of TSPO expression in the CPs and we have not quantified the relative contribution of epithelial and macrophage cells to TSPO overexpression in MS CPs *versus* non-MS controls. Therefore, it is possible that, beyond CD163+/TSPO+ macrophages, an expanded TSPO positive epithelial compartment in MS contributes to the higher ^{18}F-DPA-714 uptake in MS. Lastly, regarding the PET part of the study, we highlight that the comparison in terms of ^{18}F-DPA-714 uptake was made between only one pre-symptomatic patient (n=1) and a group of patients with MS (n=22) or HC (n=19); hence, this data needs further confirmation on a PET cohort of pre-symptomatic subjects.

In conclusion, by identifying an imaging signature in choroid plexuses already in pre-symptomatic MS, our work supports their role from the early phases of disease development, and encourages further investigations on the involvement of CP immune infiltration and BCSFB dysfunction in disease onset.

Acknowledgements

The clinical studies analyzed in this article were sponsored by APHP (Assistance Publique des Hopitaux de Paris) and have benefited from the following funding: ELA (European Leukodystrophy Association, grant 2007-0481); Programme Hospitalier de Recherche Clinique (PHRC national, 2010; APHP); INSERM-DHOS (grant 2008-recherche clinique et translationnelle); ANR (Agence Nationale de la Recherche), grant MNP2008-007125; Investissements d'avenir ANR-10-IAIHU-06. They received additional funding from Foundation ARSEP, ECTRIMS, Association France Parkinson, JNLF (Journées de Neurologie de Langue Française), FRM (Fondation pour la Recherche Médicale), and the Bouvet-Labruyére prize through the Fondation de France. This work was performed on a platform member of the France Life Imaging network (grant ANR-11-INBS-0006).

Author contributions

V.A.G.R. and B.S. conceived and designed the study. C.L., M.B., B.B. and B.S. contributed to subject enrolment and data acquisition. V.A.G.R., A.C., E.P., A.Y.P., and Em.M. analyzed the data. El.M. and D.S. performed the histology. V.A.G.R., A.L. and B.S. supervised the statistical analysis. V.A.G.R. and A.L. prepared the tables and figures. V.A.G.R. and B.S. wrote the manuscript.

Conflict of interest

The authors declare no conflict of interest related to this work.
V.A.G.R. reports fees for traveling from Novartis and Roche, personal fees form Biogen, and consulting fees from M3 Global Research and Atheneum Partners. C.L. has received consulting or travel fees from Biogen, Novartis, Roche, Sanofi, Teva and Merck Serono, none related to the present work. E.P. has received a grant for PhD fellowship from Foundation ARSEP. A.C., A.Y.P., A.L., Em.M., El.M., M.B. and D.S. report no disclosures. B.B. reports fees for traveling and speaker's honoraria from Roche, Sanofi-Genzyme, Biogen and Merck Serono, and research support from ARSEP, FISM, Roche and Biogen, all outside of the submitted work. B.S. reports grants and personal fees for lectures from Roche, Sanofi-

Genzyme, and Merck-Serono, personal fees for lectures from Novartis, Biogen and Teva, all outside of the submitted work.

References

1. Khasawneh AH, Garling RJ, Harris CA. Cerebrospinal fluid circulation: What do we know and how do we know it? *Brain Circ*. 2018;4(1):14-18.
2. Ghersi-Egea JF, Strazielle N, Catala M, Silva-Vargas V, Doetsch F, Engelhardt B. Molecular anatomy and functions of the choroidal blood-cerebrospinal fluid barrier in health and disease. *Acta Neuropathol*. 2018;135(3):337–361.
3. Johanson CE, Stopa EG, McMillan PN. The blood-cerebrospinal fluid barrier: structure and functional significance. *Methods Mol Biol*. 2011;686:101-131.
4. Ricigliano VAG, Morena E, Colombi A, et al. Choroid plexus enlargement in inflammatory multiple sclerosis: 3T MRI and translocator protein PET evaluation. *Radiology*. 2021;301(1):166-177.
5. Fleischer V, Gonzalez-Escamilla G, Ciolac D, et al. Translational value of choroid plexus imaging for tracking neuroinflammation in mice and humans. *Proc Natl Acad Sci U S A*. 2021;118(36):e2025000118.
6. Reboldi A, Coisne C, Baumjohann D, et al. C-C chemokine receptor 6-regulated entry of TH-17 cells into the CNS through the choroid plexus is required for the initiation of EAE. *Nat Immunol*. 2009;10(5):514–523.
7. Schmitt C, Strazielle N, Ghersi-Egea JF. Brain leukocyte infiltration initiated by peripheral inflammation or experimental autoimmune encephalomyelitis occurs through pathways connected to the CSF-filled compartments of the forebrain and midbrain. *J Neuroinflammation*. 2012;9:187.
8. Okuda DT, Mowry EM, Beheshtian A, et al. Incidental MRI anomalies suggestive of multiple sclerosis: the radiologically isolated syndrome. *Neurology*. 2009;72(9):800–805
9. De Stefano N, Giorgio A, Tintoré M, et al. MAGNIMS study group. Radiologically isolated syndrome or subclinical multiple sclerosis: MAGNIMS consensus recommendations. *Mult Scler*. 2018;24(2):214–221.
10. Okuda DT, Siva A, Kantarci O, et al. Radiologically isolated syndrome: 5-year risk for an initial clinical event. *PLoS One*. 2014;9(3):e90509.
11. Lebrun-Frénay C, Rollot F, Mondot L, et al. Risk Factors and Time to Clinical Symptoms of Multiple Sclerosis Among Patients With Radiologically Isolated Syndrome. *JAMA Netw Open*. 2021;4(10):e2128271.

12. Bodini B, Poirion E, Tonietto M, et al. Individual mapping of innate immune cell activation is a candidate marker of patient-specific trajectories of disability worsening in Multiple Sclerosis. *J Nucl Med*. 2020;61(7):1043-1049.
13. Owen DRJ, Gunn RN, Rabiner EA, et al. Mixed-affinity binding in humans with 18-kDa translocator protein ligands. *J Nucl Med*. 2011;52(1):24–32.
14. Lavisse S, Goutal S, Wimberley C, et al. Increased microglial activation in patients with Parkinson disease using [18 F]-DPA-714 TSPO PET imaging. *Parkinsonism Relat Disord*. 2021;82:29-36.
15. Jenkinson M, Smith S. A global optimisation method for robust affine registration of brain images. *Med Image Anal*. 2001;5(2):143–156.
16. Fischl B, Salat DH, Busa E, et al. Whole brain segmentation: automated labeling of neuroanatomical structures in the human brain. *Neuron*. 2002;33(3):341-355.
17. Yushkevich PA, Piven J, Cody Hazlett H, et al. User-guided 3D active contour segmentation of anatomical structures: Significantly improved efficiency and reliability. *Neuroimage*. 2006;31(3):1116-1128.
18. García-Lorenzo D, Lavisse S, Leroy C, et al. Validation of an automatic reference region extraction for the quantification of [18F]DPA-714 in dynamic brain PET studies. *J Cereb Blood Flow Metab*. 2018;38(2):333-346.
19. Thomas BA, Cuplov V, Bousse A, et al. PETPVC: A Toolbox for Performing Partial Volume Correction Techniques in Positron Emission Tomography. *Phys Med Biol*. 2016;61(22):7975-7993.
20. Ivan DC, Walthert S, Berve K, Steudler J, Locatelli G. Dwellers and Trespassers: Mononuclear Phagocytes at the Borders of the Central Nervous System. *Front Immunol*. 2021;11:609921.
21. Bogie JFJ, Stinissen P, Hendriks JJA. Macrophage subsets and microglia in multiple sclerosis. *Acta Neuropathol*. 2014;128(2):191-213.
22. Bodini B, Tonietto M, Airas L, Stankoff B. Positron emission tomography in multiple sclerosis - straight to the target. *Nat Rev Neurol*. 2021. doi: 10.1038/s41582-021-00537-1.Online ahead of print.
23. Rodríguez-Lorenzo S, Konings J, Van Der Pol S, et al. Inflammation of the choroid plexus in progressive multiple sclerosis: Accumulation of granulocytes and T cells. *Acta Neuropathol Commun*. 2020;8(1):9.

24. Vercellino M, Votta B, Condello C, et al. Involvement of the choroid plexus in multiple sclerosis autoimmune inflammation: A neuropathological study. *J Neuroimmunol*. 2008;199(1-2):133–141.
25. Betlazar C, Harrison-Brown M, Middleton RJ, Banati R, Liu G-J. Cellular Sources and Regional Variations in the Expression of the Neuroinflammatory Marker Translocator Protein (TSPO) in the Normal Brain. *Int J Mol Sci*. 2018;19(9):2707.
26. McMenamin PG, Wealthall RJ, Deverall M, Cooper SJ, Griffin B. Macrophages and dendritic cells in the rat meninges and choroid plexus: three-dimensional localisation by environmental scanning electron microscopy and confocal microscopy. *Cell Tissue Res*. 2003;313(3):259-269.
27. Müller J, Sinnecker t, Wendebourg MJ, et al. Choroid Plexus Volume in Multiple Sclerosis vs Neuromyelitis Optica Spectrum Disorder: A Retrospective, Cross-sectional Analysis. *Neurol Neuroimmunol Neuroinflamm*. 2022;9(3):e1147.
28. Niccolini F, Su P, Politis M. PET in multiple sclerosis. *Clin Nucl Med*. 2015;40(1):e46-52.
29. Akkus Z, Galimzianova A, Hoogi A, Rubin DL, Erickson BJ. Deep Learning for Brain MRI Segmentation: State of the Art and Future Directions. *J Digit Imaging*. 2017;30(4):449-459.
30. Schmidt-Mengin M, Ricigliano VAG, Bodini B, et al. Axial multi-layer perceptron architecture for automatic segmentation of choroid plexus in multiple sclerosis. *arXiv preprint* arXiv. 2021:2109.03778.
31. Zhao L, Taso M, Dai W, Press DZ, Alsop DC. Non-invasive measurement of choroid plexus apparent blood flow with arterial spin labeling. *Fluids Barriers CNS*. 2020;17(1):58.
32. Stilund M, Reuschlein A-K, Christensen T, et al. Soluble CD163 as a marker of macrophage activity in newly diagnosed patients with multiple sclerosis. *PLoS One*. 2014;9(6):e98588.
33. Zhang Z, Zhang Z-Y, Schittenhelm J, et al. Parenchymal accumulation of CD163+ macrophages/microglia in multiple sclerosis brains. *J Neuroimmunol*. 2011;237(1-2):73-79.

Target (abbreviated name)	Target (full name)	Type of primary antibody	Laboratory	Primary antibody reference	Buffer	Dilution	Time of exposure
CD163	Acute phase-regulated transmembrane protein on monocytes	Monoclonal (mouse)	Cell Marque®	MRQ-26	CC1®	1:50	32 min
CD20	Transmembrane protein expressed on B cells	Monoclonal (mouse)	Dako®	L26	CC1®	1:100	32 min
CD3	Epsilon chain of the human CD3	Monoclonal (rabbit)	Ventana®	2GV6	CC1® 30 min at 95°C	prediluted	32 min
CD68	Lysosomal fraction of human macrophages	Monoclonal (mouse)	Dako®	KP1	CC1®	1 :100	20 min
TSPO/PBR	Synthetic peptide peripheral type benzodiazepine receptor	Monoclonal (rabbit)	Abcam®	EPR5384	CC1®	1:10 000	36 min

Table 1. List of primary antibodies used for immunostaining. CC1 = high pH (=8) Cell Conditioning Buffer 1, supplied by Ventana Medical.

Volume	Pre-symptomatic MS	MS	HC	Pre-symptomatic MS *versus* MS	Pre-symptomatic MS *versus* HC
TIV	$15.3\pm1.9\times10^{5}$	$14.9\pm1.5\times10^{5}$	$14.7\pm1.6\times10^{5}$	$p=0.27$	$p=0.21$
Brain parenchyma	0.7±0.07	0.6±0.04	0.7±0.08	$p<0.001$	$p=0.11$
Ventricles	$16.4\pm7.1\times10^{-3}$	$20.4\pm8.2\times10^{-3}$	$12.9\pm4.7\times10^{-3}$	$p=0.03$	$p=0.009$
Choroid plexus	$14.9\pm5.2\times10^{-4}$	$15.9\pm4.5\times10^{-4}$	$11.3\pm3.9\times10^{-4}$	$p=0.35$	$p<0.001$

Table 2. Comparison of volumes of different brain regions between pre-symptomatic MS, MS and HC. Volumes were normalized on total intracranial volume (except for the first row) and expressed as mean ± standard deviation. Mean comparison between groups was performed using unpaired t-tests after normality test (Shapiro-Wilk). TIV = total intracranial volume. *p* = p-value from the t-test.

Figures

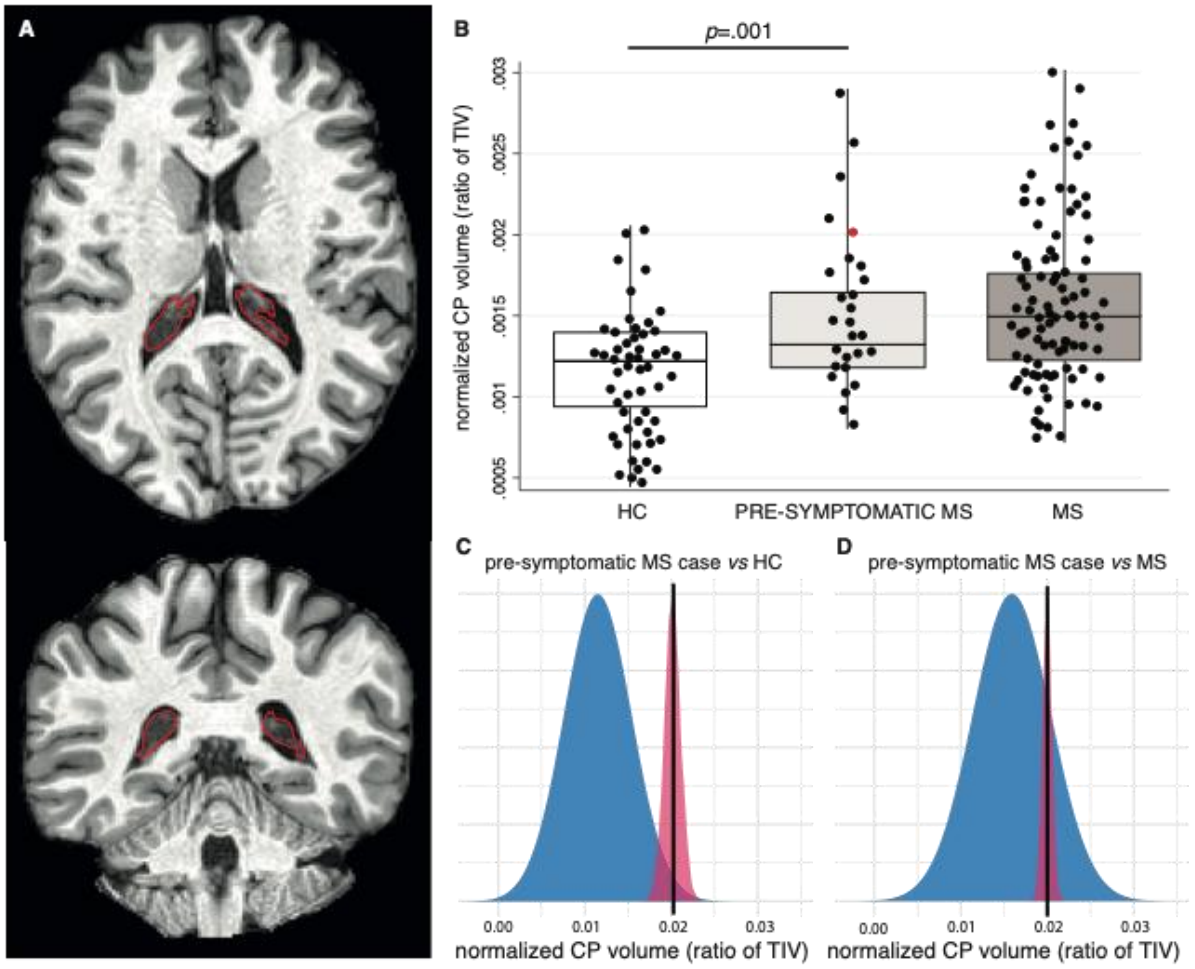

Figure 1. Enlarged CPs in pre-symptomatic MS. **A.** Unenhanced 3DT1-weighted MPRAGE images showing show segmentation of left and right CP (outlined in red) in axial (top) and coronal (bottom) planes in a pre-symptomatic MS subject. **B**. Box plots showing significantly higher CP volume in the whole pre-symptomatic MS group *versus* HC, and no difference compared with MS. CP volume was normalized according to total intracranial volume (TIV). To note, the dot corresponding to the volume of the pre-symptomatic case further examined in the PET part of this study is colored in red. Box represents interquartile range and median, whereas whiskers represent minimum and maximum values in data. The p-value corresponds to that of the multivariable linear regression model. **C-D**. Graphical illustration of the distribution of normalized CP volume in HC *versus* the single pre-symptomatic woman (**C**), and in MS versus the single pre-symptomatic woman (**D**) from the Crawford-Howell test. Note that the presence of a distribution for a single case value is based on the assumptions of the test performed and depends on the statistics of the reference cohort.

HC = healthy controls; MS = multiple sclerosis; CP = choroid plexus; TIV = total intracranial volume; p = p-value.

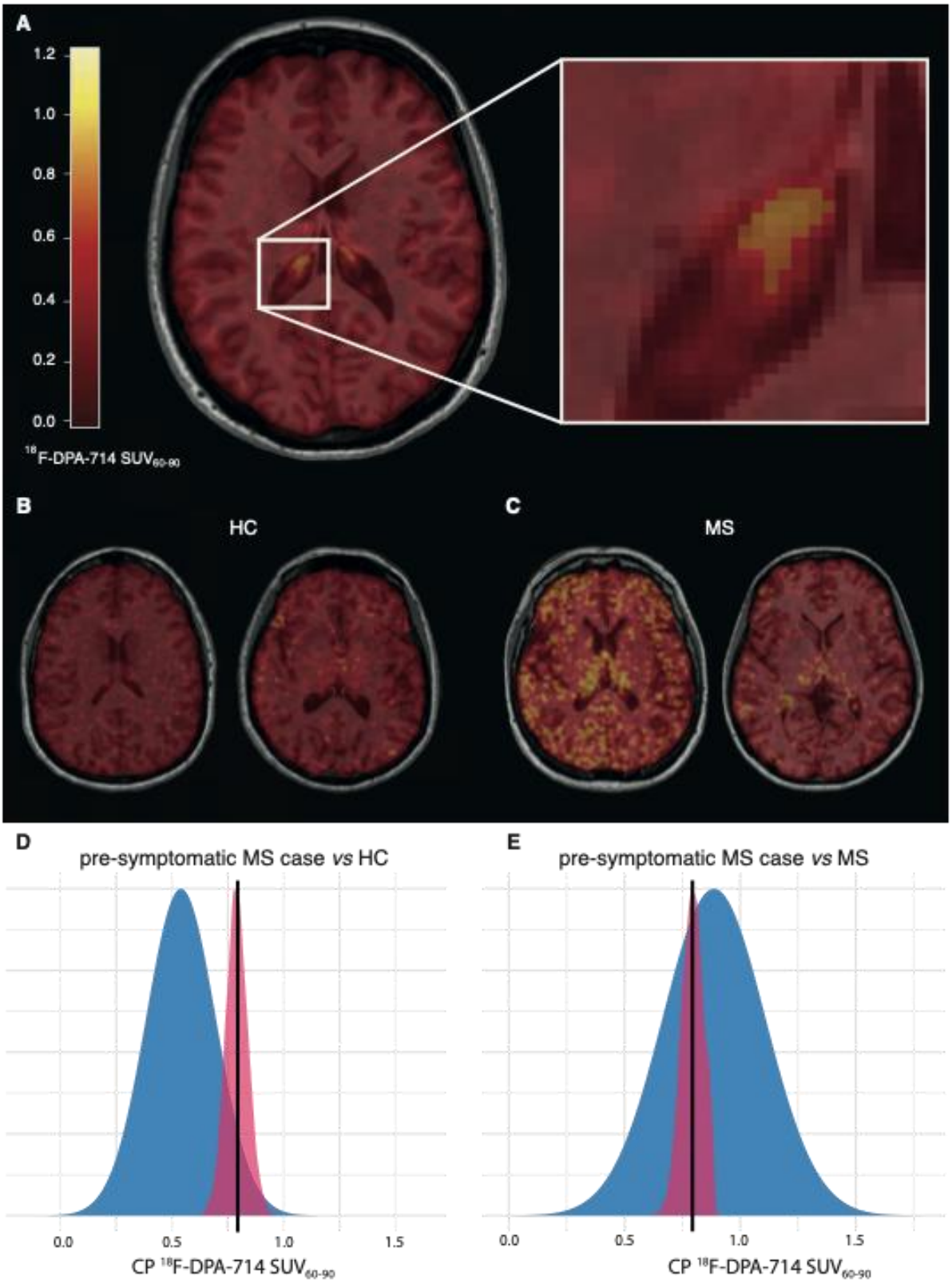

Figure 2. Higher ^{18}F-DPA-714 uptake in the CPs of pre-symptomatic MS. A. Axial ^{18}F-DPA-714 $SUV_{60\text{-}90}$ map registered onto the 3DT1-weighted MPRAGE image of the pre-symptomatic MS case, with the corresponding color bar (left), and magnification on the CP of the right lateral ventricle (right). **B-C**. Examples of axial ^{18}F-DPA-714 $SUV_{60\text{-}90}$ maps

registered onto the 3DT1-weighted MPRAGE images from two controls (**B**) and two patients with RRMS (**C**). **D**-**E**. Graphical illustration of the distribution of CP ^{18}F-DPA-714 $SUV_{60\text{-}90}$ in HC *versus* the pre-symptomatic woman (**D**), and in MS versus the pre-symptomatic woman (**E**) from the Crawford-Howell test. The presence of a distribution for a single case value is based on the assumptions of the test performed and depends on the statistics of the reference cohort. HC = healthy controls; MS = multiple sclerosis; CP= choroid plexus; TIV = total intracranial volume; $SUV_{60\text{-}90}$ = standardized uptake value between 60 and 90 minutes of acquisition; p = p-value.

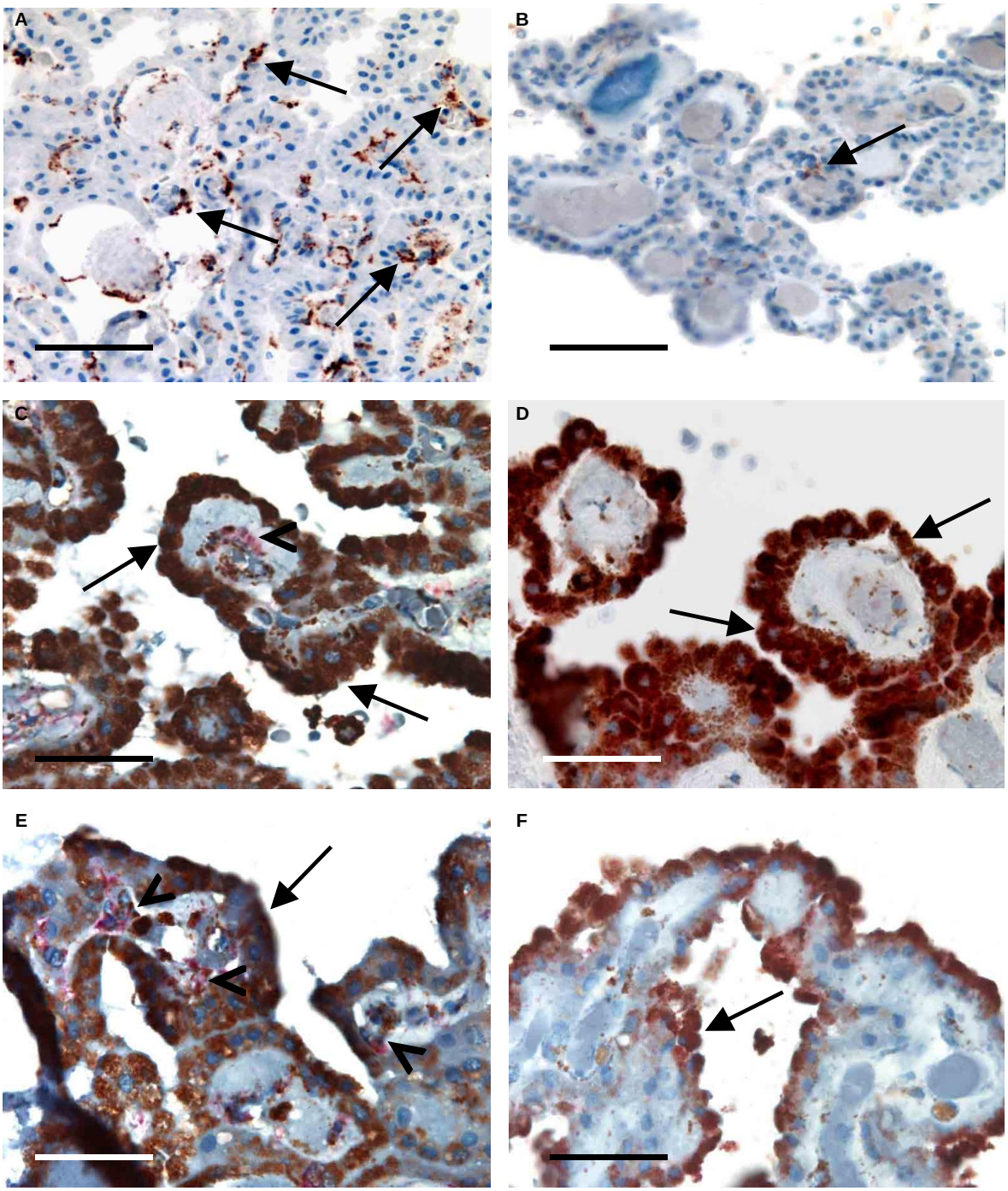

Figure 3. TSPO+/CD163+ macrophages are found in MS CPs. A-B. Excess of CD163+ macrophages (Mouse monoclonal antibody, Cell Marque®; brown, arrows) in a PPMS case (**A**) compared to a healthy control (**B**). **C-F**. TSPO (monoclonal rabbit antibody, Abcam®; brown) is highly expressed in epithelial cells (arrows) of choroid plexuses in both MS (**C**: PPMS, and **E**: SPMS) and controls (**D**: HC, **F**: epilepsy control). CD163+ (red), TSPO+ (brown) perivascular macrophages (arrowheads) are found in MS (**C, E**), but not in controls (**D, F**). Scale bars = 40 µm (**A, B**), 20 µm (**C-F**).